

Thermodynamic modeling of ion exchange resin catalyzed liquid phase esterification

Tuomo Sainio* and Erkki Paatero, Lappeenranta University of Technology, Laboratory of Industrial Chemistry, Skinnarilankatu 34, FIN-53850 Lappeenranta, Finland

* Corresponding author. E-mail: tuomo.sainio@lut.fi
Tel: +358-5-6212269, fax: +358-5-6212199

Abstract

Ion exchange resin catalyzed esterification of acetic acid with ethanol was investigated experimentally and by means of mathematical modeling. Simultaneous chemical and phase equilibrium as well as reaction kinetics were determined by using three sulfonated PS–DVB ion-exchange resins of different cross-link densities (5.5 wt-%, 7.0 wt-%, and 20 wt-%) and porosities (microporous, mesoporous, and macroporous).

The equilibrium behavior of the liquid–resin systems was correlated with a modified Flory–Huggins model, coupled with an expression for the swelling pressure in the resin phase. The reaction rate equation was written in terms of resin phase concentrations and activity coefficients. The effect of resin swelling on the H^+ ion concentration was explicitly included in the rate equation.

As to the equilibrium state of the system in a batch reactor, the selective sorption effect (i.e., lower concentration of water than of ethyl acetate in the liquid phase) was found to decrease with increasing cross-link density of the resin. The thermodynamic model was able to reproduce this phenomenon. Further, the model predicted that the fractional extent of reaction in a batch reactor increases with the amount of resin catalyst in the system.

In the kinetic experiments it was found that the overall reaction rate per unit mass of resin catalyst decreases with increasing cross-link density, which is in accordance with the previous works. However, it was shown that this phenomenon does not stem from decreasing accessibility of the sulfonic acid groups, which is the classical explanation, but is linked to the phase equilibrium behavior of the reactive system containing an elastic polymeric component.

Introduction

Two phenomena are characteristic for ion-exchange resins in catalytic applications. Firstly, the cross-linked polymer network may swell to a variable extent depending on the external liquid phase composition, the affinity of the polymer for the solvents, and the amount of cross-links in the polymer [1]. Secondly, owing to the selective sorption capability of the resin, the reactants are not necessarily present in stoichiometric proportions in the reaction locus.

At low swelling ratios of the resin, part of the sulfonic acid groups may be totally unreachable by the reactants due to steric hindrance. Poor *accessibility* of the functional groups, as this phenomenon is known, naturally diminishes experimentally observed reaction rates. It is often reported that increasing the cross-link density of gel-type resins leads to decreasing accessibility [2]. The *catalytic activity* of the functional groups is known to vary

depending on the conditions [3]. If the reaction is carried out in a non-polar medium where one or more of the products is highly polar (such as water), adsorption of the product molecules on the functional group may inhibit the reaction [4]. Moreover, it has been shown that the reaction may stop before the thermodynamic equilibrium has been attained due to “deactivation” of the resin catalyst by strongly bound water molecules [5].

The modeling approaches applied in the literature to kinetic modeling of ion-exchange resin catalyzed esterification of carboxylic acids with alkanols and ester hydrolysis reactions fall into three categories. The *pseudo-homogeneous approach* is often applicable in excess of a polar solvent, such as water, since the counter-ions are then solvated and mobile. *Adsorption models* (Eley–Rideal, Langmuir–Hinshelwood–Hougen–Watson, etc.) are mainly used in presence of non-polar solvents, where the undissociated functional group of the resin serves as the adsorption site.

The essence of *heterogeneous two-phase models* is that the ion-exchange resin is seen as a cross-linked polymer solution, surrounded by an external fluid phase. The reaction mixture components partition between these phases as governed by thermodynamics. Thermodynamic models derived for polymer solutions and gels have recently been applied in describing the reaction kinetics and equilibria in multicomponent liquid mixture–ion-exchange resin systems for a number of reactions [6 – 9], and will be used in this work as well.

Materials and methods

Three sulfonated poly(styrene-co-divinylbenzene) (PS-DVB) cation-exchange resins with different cross-link densities and porosities were used in the experiments. The resins are referred to with codes shown in Table 1. X5½ is a standard gel type (microporous) resin, whereas X20 is a standard macroporous, highly cross-linked resin. X7 is a mesoporous resin with a moderate degree of cross-linking. The physical properties of the resins are given in Table 1.

Modeling

Table 1. Properties of the ion-exchange resins in the H⁺ form.

Property	X5½	X7	X20
Trade name	CS11GC	KEF76	Amberlyst 15
Manufacturer	Finex Oy	Finex Oy	Rohm & Haas
Cross-link density, wt-%	5.5	7.0	20
Particle size in water, mm	0.32	0.3	0.4 – 0.7
Macroporosity, vol-%	0	7	35
Ion-exchange capacity, equiv kg ⁻¹	5.1	5.1	5.1
Specific volume of the polymer, m ³ kg ⁻¹	6.54·10 ⁻⁴	6.71·10 ⁻⁴	6.87·10 ⁻⁴
Degree of functionalization, %	95	95	97
Repeating units in polymer, mol kg ⁻¹	5.48	5.48	5.36

The esterification reaction between acetic acid (HOAc) and ethanol (EtOH) produces ethyl acetate (EtOAc) and water, as shown in Eq. (1). In what follows, the activity model and the reaction kinetic model used are presented. For a more detailed derivation of the activity model the reader is referred to Sainio *et al.* [10].



Activity model

Ion-exchange resins are cross-linked polyelectrolytes. The presence of the charged groups as well as the limited expansibility of the material should therefore be taken into account in the activity model. The entropic contribution of the dissociated counter-ions is here modeled in the framework of Manning's counter-ion condensation theory [11, 12], whereas electrostatic interactions between the liquid components and the polymer are implicitly included in the adjustable parameters of the model.

According to the counter-ion condensation theory, the free energy of a polyelectrolyte solution attains its minimum value when a fraction of the counter-ions is dissociated and free, while the rest is "topologically condensed" close to the polymer matrix. Furthermore, there exists a well defined minimum distance, equal to the Bjerrum length, between two adjacent dissociated groups in the polymer matrix. Although the condensed counter-ions are not covalently bound to the functional group, they renormalize the line charge density of the polyelectrolyte to a threshold value, which depends on temperature and the dielectric properties of the solvent environment [11]. In the current context, the important property of the condensed counter-ions is that they do not contribute to the mixing entropy of the system, but are an inseparable part of the polymer structure. According to the counter-ion condensation theory, the amount of dissociated (free) counter-ions is obtained from Eq. (2). Their volume fraction in the polymer solution was approximated by Eq. (3).

$$n_c = 4\pi n_m DF \varepsilon_0 \varepsilon k_b T \delta / z e_0^2 \quad (2)$$

$$\phi_c \approx \phi_p m_{cm} n_c / n_m \quad (3)$$

It should be noted that as the extent of swelling of an ion-exchange resin increases, the configurational entropy of the polymer network decreases. This brings about a tensile force that opposes the expansion of the resin, and which is observed as an increase in the pressure of the resin phase. Consequently, there exists a pressure difference (swelling pressure, π_{sw}) between the resin phase and the external liquid phase.

The expression used for calculating the swelling pressure was derived from the three-chain model of elastic networks [13, 14], and is shown in Eq. (4). In this model, the chain length distribution of the polymer is described using the Langevin distribution function. The extent of swelling was calculated based on the density of the polymer, which was determined in the water-swollen state by means of a pycnometer.

$$\pi_{sw} = \frac{1}{3} K_{el} \phi_p^{2/3} N_{stat}^{1/3} \mathcal{L}^{-1}(\gamma), \quad \gamma = \phi_p^{-1/3} N_{stat}^{-1/2} \quad (4)$$

The activity coefficients of the reaction mixture components were calculated with an extended Flory–Huggins activity model shown in Eq. (5) [10]. In contrast with the original model, the interaction parameters were taken as concentration dependent as shown in Eqs. (6) and (7).

$$\begin{aligned} \ln a_i^p(p^p) = & 1 + \ln \phi_i^p - \sum_{j=1}^{NP+1} m_{ij} \phi_j^p + \sum_{j=1}^{NP} \chi_{ij} \phi_j^p - \sum_{j=1}^{NP} \sum_{k=1}^{j-1} m_{ik} \chi_{kj} \phi_k^p \phi_j^p \\ & - \sum_{j=1}^{NP-1} u_i^j u_j^j \phi_j^p \frac{\partial \chi_{ij}}{\partial u_j^j} - \sum_{j=1}^{NP-1} m_{ij} \phi_j^p \phi_p^2 \frac{\partial \chi_{jp}}{\partial \phi_p} \\ & + \frac{9}{4\epsilon} (p_i - p') (m_{ic} \phi_c (\ln \phi_c + 1)) \left(1 + (1 + 9p') \left(\sqrt{(1 + 9p')^2 + 8} \right)^{-1} \right) \\ & + V_{m,i} \pi_{sw} / R_g T \end{aligned} \quad (5)$$

$$\chi_{ij}(T, u) = \chi_{ij}^0 + b_{ij} u_j^j + (a_{ij} + c_{ij} u_j^j) / T \quad (6)$$

$$\chi_{ip}(T, \phi) = \chi_{ip}^0 + b_{ip} \phi_p + (a_{ip} + c_{ip} \phi_p) / T \quad (7)$$

A reduced volume fraction, defined as $u_i^j = \phi_i / (\phi_i + \phi_j)$, was used as the concentration variable for the solvent–solvent interaction parameter, whereas ϕ_p was used for the solvent–polymer interactions. The following relationships hold for the parameters in Eq. (6): $\chi_{ji}^0 = m_{ji}(\chi_{ij}^0 + b_{ij})$, $a_{ji} = m_{ji}(a_{ij} + c_{ij})$, $b_{ji} = -m_{ji}b_{ij}$, and $c_{ji} = -m_{ji}c_{ij}$. The molecular size ratio m_{ij} was calculated from the pure component molar volumes according to $m_{ij} = V_{m,i} / V_{m,j}$. The parameter m_{ip} may be taken as zero because the molecular size of the polymer is large compared to that of the liquid components.

The same activity model was used also in the liquid phase by setting ϕ_p equal to zero. The index $NP+1$ in the summations refers to the dissociated counter-ions.

Reaction kinetics

The uncatalyzed esterification reaction is known to proceed at a very low rate [15], and was therefore neglected here. Since the reaction is considered to occur in a polymer solution, the reaction rate is proportional to the concentration of the H^+ ions, which depends on the ion-exchange capacity of the resin and varies with the extent of swelling of the particles. The reaction rate can thus be written as shown in Eq. (8).

$$r^S = k_1 \frac{q \rho_p}{\theta} C_{EtOH}^S C_{HOAc}^S \left(1 - \frac{1}{K_a^S} \prod_{j=1}^N a_j^{\nu_j} \right) \quad (8)$$

The reaction equilibrium constant in the resin phase is obtained from the reaction Gibbs energy, corrected for the swelling pressure as illustrated in Eq. (9). The temperature dependency of the reaction rate constants was described with the Arrhenius equation.

$$K_a^S = \exp\left(-\frac{\Delta_R G(p^L)}{R_g T} - \frac{\pi_{sw}}{R_g T} \sum_{j=1}^N v_j V_{m,j}\right) \quad (9)$$

Reaction and diffusion in swelling/shrinking resin

It should be noted that the resin particles could swell or shrink during a chemical reaction owing to differences in the affinities of the products and reactants to the resin. This should be taken into account when formulating the intraparticle mass transfer model. Fickian particle diffusion coupled with a single chemical reaction in homogeneous, spherical particles can be described with Eqs. (10) and (11) [9, 16]. A transformed coordinate system, namely polymer mass coordinates, is used as the frame of reference in order to keep the spatial domain invariant during the calculations.

$$\frac{\partial C_i^S}{\partial t} = \frac{\rho_p^2}{\theta} \frac{\partial}{\partial W} \left(\frac{D_i^S A^2}{\theta} \frac{\partial C_i^S}{\partial W} \right) + v_i r^S - \frac{C_i^S}{\theta} \frac{\partial \theta}{\partial t} \quad (10)$$

$$\frac{\partial \theta}{\partial t} = \sum_j V_{m,j} \left(\rho_p^2 \frac{\partial}{\partial W} \left(\frac{D_j^S A^2}{\theta} \frac{\partial C_j^S}{\partial W} \right) + v_j r^S \theta \right) \quad (11)$$

Batch reactor model

The liquid phase composition in a finite-volume batch reactor is obtained by integrating Eqs. (12) and (13), where V^L denotes the volume of the liquid phase, n is number of moles, and N_p is the number of (monodisperse) particles in the reactor. W_p refers to the mass of a single particle. Liquid phase mass transfer effects were neglected because they were found to be insignificant in non-reactive sorption kinetics experiments [9], the characteristic time of which shorter than that of the esterification reaction. The decrease in the liquid phase volume due to sampling was taken in to account in the calculations.

$$\frac{\partial C_i^L}{\partial t} = \frac{1}{V^L} \frac{\partial n_i^L}{\partial t} - C_i^L \sum_j V_{m,j} \frac{\partial n_j^L}{\partial t} \quad (12)$$

$$\frac{\partial n_i^L}{\partial t} = -N_p \rho_p \left(\frac{D_i^S A^2}{\theta} \frac{\partial C_i^S}{\partial W} \right)_{W=W_p} \quad (13)$$

Parameter estimation

The Flory–Huggins interaction parameters used in Eq. (5) are given in Table 2. As regards the liquid components, the parameter values were estimated from isobaric vapor–liquid equilibrium data in the literature, except for the reactive pairs water–EtOAc and EtOH–HOAc, for which such data is not as readily available. In these two cases the parameter values were estimated from the simultaneous chemical and phase equilibrium measurements (see below).

Table 2. Flory–Huggins interaction parameters for the solvent–solvent pairs and between the solvents and the X5½, X7, and X20 ion-exchange resins in H⁺ form.

Component		Interaction parameters			
<i>i</i>	<i>j</i>	χ_{ij}^0	b_{ij}	a_{ij}	c_{ij}
water	ethanol	1.5673	−0.4307	−273.47	337.26
	acetic acid	0.3166	0.3576	60.583	41.414
	ethyl acetate ¹⁾	0.662	1.491	–	–
	resin	−0.6342	0.8612	–	–
ethyl acetate	ethanol	−0.5137	−0.1661	727.16	−168.64
	acetic acid	0.7668	0.5586	−3.9038	−370.10
	resin	−0.0866	−0.8375	–	–
ethanol	acetic acid ¹⁾	−0.847	−1.163	–	–
	resin	−2.4688	0.0011	–	–
acetic acid	resin	−0.0118	−0.0056	–	–

¹⁾ Estimated from reactive phase equilibrium data for resin catalyzed esterification of acetic acid with ethanol.

The liquid–polymer interaction parameters were estimated from binary sorption isotherms (see Sainio [9] for details). Identical parameters were used for all ion-exchange resins. It should be noted that the data set used covers the whole composition range of all of the non-reactive binary pairs and is not limited to the case of equimolar mixture of the reactants. As seen in Table 2, the effect of temperature on the liquid–polymer Flory–Huggins interaction parameters was neglected because of lack of suitable data.

The swelling pressure model has two adjustable parameters, namely the elastic coefficient and the number of statistical segments. These were estimated from the same non-reactive binary sorption experiments as the liquid–polymer Flory–Huggins interaction parameters. The parameter values are given in Table 3.

The thermodynamic reaction equilibrium constant was not estimated from the simultaneous chemical and phase equilibrium data but was calculated from literature values for the Gibbs energy of formation [17]; a value of $\Delta_R G = -6.587 \text{ kJ mol}^{-1}$ was used.

The forward reaction rate constant, k_1 , was the only parameter estimated from the kinetic experiments at each temperature. The sorption selectivity of the resin makes it difficult to determine the extent of reaction in a batch reactor. Therefore, the liquid phase mole fractions of all four components were used as state variables in estimating the kinetic parameters. The Arrhenius equation parameters, *i.e.* pre-exponential factor and the activation energy of the reaction, were calculated from k_1 values obtained at different temperatures. The reaction kinetic parameters are listed in Table 4.

Table 3. Parameters of the non-Gaussian elasticity model, Eq. (4), estimated for the X5½, X7, and X20 ion-exchange resins in H⁺ form.

Resin	K_{el} , MPa	N_{stat}
X5½	4.637	2.546
X7	4.203	2.237
X20	4.012	1.454

Table 4. Esterification reaction rate constants and Arrhenius equation parameters for liquid phase esterification of acetic acid with ethanol catalyzed by X5½, X7, and X20 ion-exchange resins in H⁺ form.

Resin	$k_1, 10^{-10} \text{ m}^6 \text{ mol}^{-2} \text{ s}^{-1}$			$E_{\text{act}}, \text{kJ mol}^{-1}$	$A, \text{m}^6 \text{ mol}^{-2} \text{ s}^{-1}$
	$T = 293 \text{ K}$	$T = 308 \text{ K}$	$T = 323 \text{ K}$		
X5½	0.51	1.51	5.57	62.5	6.65
X7	0.50	1.71	5.11	61.0	3.80
X20	0.45	1.54	5.34	64.7	15.1

Results and discussion

Simultaneous chemical and phase equilibrium

The effect of the amount of resin catalyst on the liquid phase composition at equilibrium in a batch reactor is illustrated in Figure 1. As seen in the figure, the selective sorption of the resin has a remarkable effect on the liquid phase composition. The effect naturally increases as the liquid to catalyst mass ratio decreases. Of the three ion-exchange resins studied, the one with the lowest cross-link density has the largest influence on the equilibrium composition. This seems to contradict with the effect of cross-link density on the sorption selectivity [10]. However, because of the simultaneous chemical and phase equilibrium, the amount of ion-exchange resin in a batch reactor has a twofold effect on the equilibrium composition.

Firstly, an increase in the weight fraction of the polymer in the system increases the departure of the liquid phase from the stoichiometric composition due to the selective sorption. In the present case, the resin preferentially sorbs water, whereas ethyl acetate tends to desorb to the liquid phase.

Secondly, the fractional extent of reaction may be different from the value obtained with a homogeneous acid catalyst due to the solvent–polymer interactions. In fact, it was shown by Sainio et al. [10] that the thermodynamic model used here predicts that, in a batch reactor, the extent of reaction may be as much as 20 % higher in presence of an ion-exchange resin catalyst than in presence of a homogeneous catalyst. Therefore, the molar amounts of ethyl acetate and water in the system are higher than with resins of lower cross-link density, and the liquid mixture becomes more non-ideal. It appears that energetic interactions overcome the effects of the cross-link density and molar volume differences on the sorption selectivity.

Batch reactor kinetics

Typical results from the reaction kinetics experiments in batch reactors with the X5½, X7, and X20 resins are displayed in Figure 2. Also these data clearly demonstrate the selective sorption effect: the products are not present in stoichiometric proportions in the liquid phase. The agreement between the experimental and calculated kinetics curves is satisfactory considering that the parameters of the thermodynamic model are obtained from independent data.

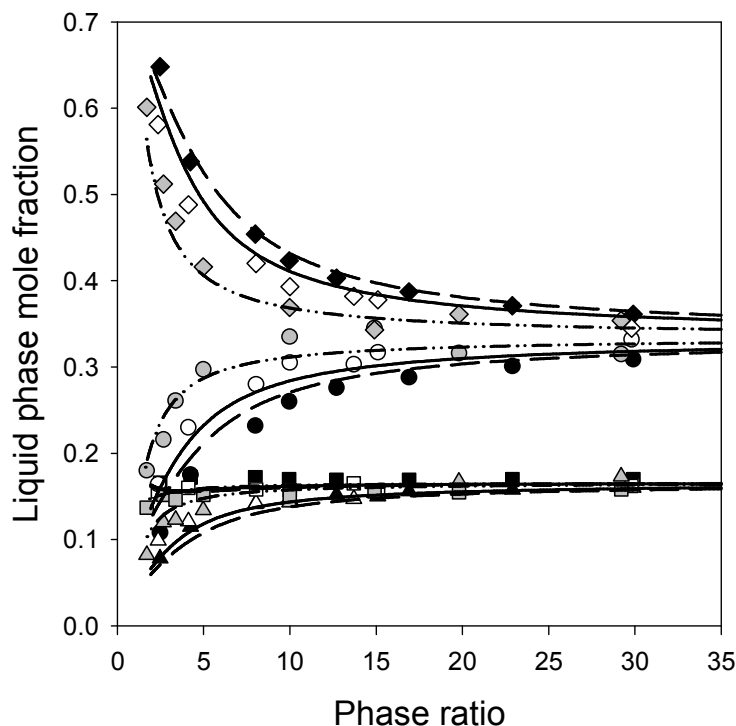


Figure 1. Simultaneous chemical and phase equilibrium in batch reactor. Esterification of acetic acid with ethanol catalyzed by X5½(H⁺) (filled symbols, - - -), X8(H⁺) (open symbols, ———), and X20(H⁺) (gray symbols, - · - · -) ion-exchange resins at 298 K. Symbols: □ = acetic acid, Δ = ethanol, ○ = water, ◇ = ethyl acetate. Acetic acid to ethanol mole ratio is equal to one in all experiments.

The reaction kinetic parameters are shown in Table 4 above. The activation energies obtained for all resins compare well with the values of 58.6 kJ/mol and 66.1 kJ/mol reported by Sardin and Villermaux [18] and Mazzotti *et al.* [7]. Typical activation energies of diffusion in swollen ion-exchange resins are in the order of 15 kJ/mol, which suggests that mass transfer effects are not significant. In non-reactive sorption kinetics experiments (not shown) it was observed that the characteristic time for diffusion in these resins is in the order of minutes and is thus much shorter than that of the chemical reaction.

As seen in Figure 2, the overall reaction rate decreases with increasing cross-link density of the resin. A similar observation was made, among others, by Rodrigues and Setínek [162], who studied transesterification of ethyl acetate with 1-propanol using gel-type resins. The authors qualitatively explained their results in terms of accessibility of the sulfonic acid groups, which was claimed to be lower for highly cross-linked resins due to smaller mesh width of the polymer network. They did not, however, take into account the resin phase concentrations of the reactants and the H⁺ ions, or the volume of the resin phase that also depends on the cross-link density. If all other parameters remain constant, a lower swelling ratio means higher proton concentration but lower concentrations of the reactants. These effects are included in Eq. (8). Consequently, the differences in the k_1 values for different resins in Table 4, are less than 7 % at each temperature. It can thus be concluded that the accessibility of the functional groups is not a critical factor for the esterification reaction studied. Instead, the lower overall reaction rate per unit mass of dry catalyst observed with

highly cross-linked resins originate from the smaller volume of the resin phase and lower concentrations of the reactants in it.

This point is further illustrated in Figure 3 where the reaction rates calculated according to Eq. (8) are plotted as a function of the extent of reaction. The same value of the rate constant was used for all resins regardless of the cross-link density, and diffusion coefficients were set large enough to eliminate the effect of mass transfer on the reaction rate. If a given mass of dry resin catalyst is charged into a batch reactor, the rate at which the products are formed is substantially higher for resins of lower cross-link density (Figure 3A). Similarly, if a fixed-bed reactor is packed with a given volume of the swollen resin, a lower cross-link density leads to higher productivity (Figure 3B), but the effect of cross-link density is not as large as in the case of constant catalyst mass. Moreover, resins of high porosity have a lower total volume of the polymer phase in a fixed-bed reactor, which further decreases the overall reaction rate in a fixed-bed reactor.

It is therefore beneficial to use ion-exchange resins of low cross-link density and porosity in fixed-bed reactors, provided that the mechanical stability of the material is not an issue.

Conclusions

Ion-exchange resin catalyzed esterification of acetic acid was investigated experimentally and by means of mathematical modeling. The ion-exchange resin was treated as a cross-linked polymer solution. The partitioning of the reaction mixture components

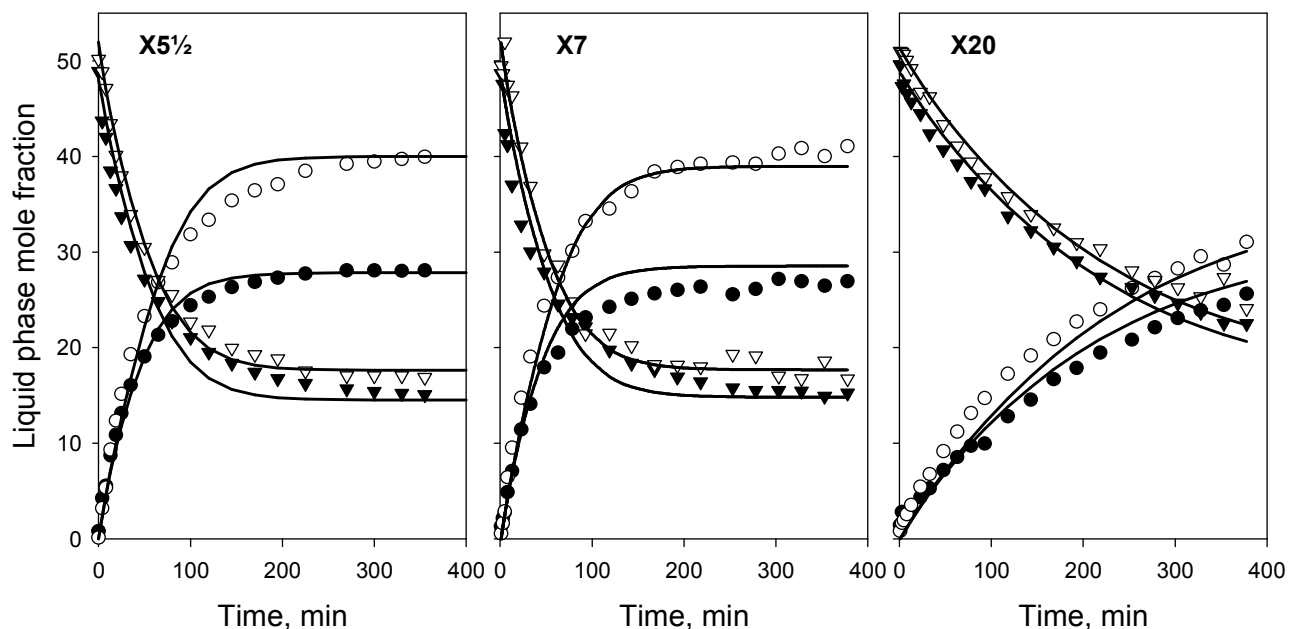


Figure 2. Kinetics of ion-exchange resin catalyzed esterification of acetic acid with ethanol. $T = 308$ K. Liquid to resin mass ratios: $X_{5\frac{1}{2}} = 8.3$, $X_7 = 8.5$, $X_{20} = 8.7$. Symbols: (\blacktriangledown) ethanol, (\triangledown) acetic acid, (\bullet) water, (\circ) ethyl acetate. Lines are calculated with the thermodynamic reaction kinetics model.

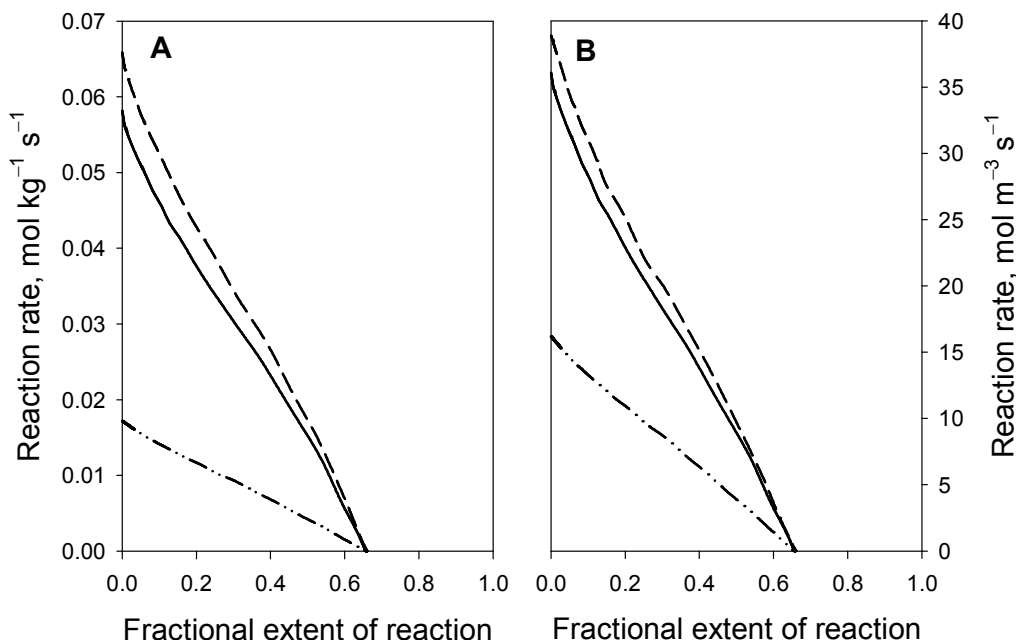


Figure 3. Effect of cross-link density on the polymer phase reaction rate per unit mass of polymer (A) and unit volume of swollen resin (B). (---) = X5½; (—) = X7; (-·-·-) = X20. Calculation parameters: $T = 323\text{K}$, $k_1 = 5.57 \cdot 10^{-10} \text{ m}^6 \text{ mol}^{-2} \text{ s}^{-1}$, and $\square_{\text{R}}G = -6.587 \text{ kJ mol}^{-1} \text{ K}^{-1}$. EtOH to HOAc mole ratio = 1, liquid to resin mass ratio = 10.

between resin and liquid phases was calculated with an activity model derived from thermodynamics of polymer solutions and gels. The presence of the dissociable charged groups, as well as the limited expansibility of the polymer network, was explicitly taken into account in the model.

In accordance with previous reports, it was found that the overall reaction rate per unit mass of resin decreases as the cross-link density of the resin increases. However, it was shown that this effect should be mainly attributed to the phase equilibrium behavior of the system rather than limited accessibility of the functional groups, which is the classical explanation.

Nomenclature

<i>A</i>	Cross-sectional area, m^2
	Pre-exponential factor, $\text{m}^6 \text{ mol}^{-2} \text{ s}^{-1}$
<i>a</i>	Activity, –
	Temperature coefficient, K
<i>b</i>	Concentration dependency parameter, –
<i>C</i>	Molar concentration, mol m^{-3}
<i>c</i>	Temperature coefficient, K
<i>D</i>	Fickian diffusion coefficient, $\text{m}^2 \text{ s}^{-1}$

DF	Degree of functionalization of the polymer
E_{act}	Activation energy, J mol^{-1}
e_0	Elementary charge, C
K_a	Thermodynamic reaction equilibrium constant, –
K_{el}	Elastic coefficient, Pa
k_1	Forward reaction rate constant, $\text{m}^6 \text{mol}^{-2} \text{s}^{-1}$
k_b	Boltzmann constant, $1.381 \cdot 10^{-23} \text{ J K}^{-1}$
\mathcal{L}^{-1}	Inverse Langevin function, –
m	Molecular size ratio, –
N_{stat}	Number of statistical segments between cross-links, –
NP	Number of components in polymer phase, –
N_p	Number of particles, –
n	Number of moles, mol
p	Polarization per unit volume, –
	Pressure, Pa
p'	Polarization of a liquid mixture per unit volume, –
q	Ion-exchange capacity, mol kg^{-1}
R_g	Gas constant, $8.314 \text{ J mol}^{-1} \text{ K}^{-1}$
r	Reaction rate, $\text{mol m}^{-3} \text{ s}^{-1}$
T	Temperature, K
t	Time, s
u	Reduced volume fraction, –
V	Volume, m^3
V_m	Molar volume, $\text{m}^3 \text{mol}^{-1}$
W	Spatial variable in mass coordinates, kg
z	Counter-ion valence, –
γ	Fractional extension of segments between cross-links, –
$\Delta_{\text{R}}G$	Gibbs energy of reaction, J mol^{-1}
ε	Dielectric constant, –
ε_0	Permittivity of vacuum, $8.854 \cdot 10^{-12} \text{ C}^2 \text{ N}^{-1} \text{ m}^{-2}$
ϕ	Volume fraction of a component, –
δ	Contour length between adjacent charged groups, m
θ	Swelling ratio, –
ν	Stoichiometric coefficient, –
π_{sw}	Swelling pressure, Pa
ρ	Density, kg m^{-3}
χ	Flory–Huggins interaction parameter, –

Superscripts

L	Liquid phase
P	Polymer phase, resin phase, solid phase
S	Polymer phase, resin phase, solid phase

Subscripts

c	Counter-ion
i,j,k	Chemical species
m	Repeating unit of the polymer
p	Polymer

References

1. Helfferich, F., *Ion-exchange*, Dover Publications, New York, 1995
2. Rodrigues, O., Setínek, K., Dependence of Esterification Rates on Crosslinking of Ion-Exchange Resins Used as Solid Catalyst, *J. Catal.*, 39(1975), 449-455
3. Buttersack, C., Widdecke, H., Klein, J., Sulfonic Acid Ion-Exchange Resins as Catalysts in Nonpolar Media. II. Influence of Conditioning Methods on the Acidity and Catalytic Activity, *React. Polym.*, 5(1987), 181-189
4. du Toit, E., Nicol, W., The Rate Inhibiting Effect of Water as a Product on Reactions Catalysed by Cation Exchange Resins: Formation of Mesityl Oxide from Acetone as Case Study, *Applied Catal. A*, 277(2004), 219-225
5. du Toit, E., Schwarzer, R., Nicol, W., Acetone Condensation on a Cation Exchange Resin Catalyst: the Pseudo Equilibrium Phenomenon, *Chem. Eng. Sci.*, 59(2004), 5545-5550
6. Lode, F., *A Simulated Moving Bed Reactor (SMBR) for Esterifications*, Diss. ETH Nr. 14350, Shaker Verlag, Aachen, 2002
7. Mazzotti, M., Neri, B., Gelosa, D., Kruglov, A., Morbidelli, M., Kinetics of Liquid-Phase Esterification Catalyzed by Acidic Resins, *Ind. Eng. Chem. Res.*, 36(1997), 3-10
8. Musante, R. L., Grau, R. J., Baltanás, M. A., Kinetic of Liquid-phase Reactions Catalyzed by Acidic Resins: the Formation of Peracetic Acid for Vegetable Oil Epoxidation *Applied Catalysis A: General* 197(2000), 165-173
9. Sainio, T., *Ion-exchange resins as stationary phase in reactive chromatography*, Diss. Lappeenranta University of Technology, Acta Universitatis Lappeenrantaensis 218, Lappeenranta, 2005
10. Sainio, T., Laatikainen, M., Paatero, E., Phase Equilibria in Solvent Mixture–Ion-exchange Resin Catalyst Systems, *Fluid Phase Equilib.*, 218(2004), 269-283
11. Manning, G. S., Limiting Laws and Counterion Condensation in Polyelectrolyte Solutions. I. Colligative Properties, *J. Chem. Phys.*, 51(1969), 924-933
12. Manning, G. S., Ray, J., Counterion Condensation Revisited, *J. Biomol. Struct. & Dyn.*, 16(1998), 461-476
13. Tiihonen, J., Markkanen, I., Kärki, A., Äänismaa, P., Laatikainen, M., Paatero, E., Modelling the Sorption of Water–Ethanol Mixtures in Cross-linked Ionic and Neutral Polymers, *Chem. Eng. Sci.*, 57(2002), 1885-1897

14. Hasa, J., Ilavský, M., Dusek, K., Deformational, Swelling, and Potentiometric Behavior of Ionized Poly(methacrylic Acid) Gels. I. Theory, J. Polym. Sci., Polym. Phys. Ed. 13(1975), 253-262
15. Arnikar, H. J., Rao, T. S., Bodhe, A. A., Gas Chromatographic Study of the Kinetics of the Uncatalyzed Esterification of Acetic Acid by Ethanol, J. Chromatogr. 47(1970), 265-268.
16. Sainio, T., Paatero, E., Modeling of diffusion and chemical reactions in ion-exchange resins, AIChE 2005 proceedings CD, New York, NY: AIChE 2005
17. *TRC Thermodynamic Tables: Non-hydrocarbons*, Thermodynamics Research Center, Texas A&M University, College Station, TX, 1996
18. Sardin, M., Villermaux, J., Estérification Catalysée par une Résine Échangeuse de Cation dans un Réacteur Reacteur Chromatographique, Nouv. J. Chim., 21(1979), 255-261